Available online at www.sciencedirect.com
SCIENCE DIRECT
Biochemical and Biophysical Research Communications 339 (2006) 226–231
BBRC
www.elsevier.com/locate/ybbrc

Tissue Prx I in the protection against Fe-NTA and the reduction of nitroxyl radicals ☆

Junya Uwayama [a,1], Aki Hirayama [b,1], Toru Yanagawa [c,1], Eiji Warabi [a], Rika Sugimoto [a], Ken Itoh [a], Masayuki Yamamoto [a], Hiroshi Yoshida [c], Akio Koyama [b], Tetsuro Ishii [a,*]

[a] *Biomolecular and Integrated Medical Sciences, Graduate School of Comprehensive Human Sciences, University of Tsukuba, Ibaraki, Japan*
[b] *Medical Sciences for Control of Pathological Processes, Graduate School of Comprehensive Human Sciences, University of Tsukuba, Ibaraki, Japan*
[c] *Functional and Regulatory Medical Sciences, Graduate School of Comprehensive Human Sciences, University of Tsukuba, Ibaraki, Japan*

Received 26 October 2005
Available online 10 November 2005

Abstract

Peroxiredoxin I (Prx I) is a key cytoplasmic peroxidase that reduces intracellular hydroperoxides in concert with thioredoxin. To study the role of tissue Prx I in protection from oxidative stress, we generated Prx $I^{-/-}$ mice by gene trapping. We then evaluated the acute-phase tissue damage caused by ferric-nitrilotriacetate (Fe-NTA). Increases in serum aspartate aminotransferase and alanine aminotransferase levels were significantly greater in Prx $I^{-/-}$ than wild-type mice, 4 and 12 h after the injection of Fe-NTA. Using real-time EPR imaging, we examined the reduction of the stable paramagnetic nitroxyl radical 3-carbamoyl-2,2,5,5-tetramethylpyrrolidine-1-oxyl in vivo, and found that the half-life of this spin probe in the liver and kidney was significantly prolonged in the Prx $I^{-/-}$ mice. These results demonstrate that Prx $I^{-/-}$ mice have less reducing activity and are more susceptible to the damage mediated by reactive oxygen species in vivo than wild-type mice.

Keywords: Ferric-nitrilotriacetate; EPR imaging; Peroxiredoxin I; Carbamoyl-PROXYL; Free radicals; OmniBank

Reactive oxygen species (ROS) and reactive nitrogen species contribute significantly to disease pathologies, such as ischemia–reperfusion injury, pulmonary oxygen toxicity, atherosclerosis, radiation effects, chemotherapeutic effects, mutagenesis, and carcinogenesis, and to aging [1]. ROS are produced constantly but are subsequently eliminated in vivo. In addition to superoxide dismutase, catalase, and glutathione peroxidase, the peroxiredoxin (Prx) family, comprised of six isoforms in mammals, plays an important role in eliminating ROS. Prx catalyzes the reduction of H_2O_2, alkyl hydroperoxides, and peroxinitrite using reducing equivalents provided by thiol-containing proteins, such as thioredoxin [2–5]. The Prx isoforms share a common reactive cysteine residue in their N-terminal region, which is oxidized to either cysteine sulfenic acid or disulfide, both of which are then readily reduced back to the sulfhydryl state by various cellular reductants [6]. Prx I is the major cytosolic Prx isoform and is expressed ubiquitously in tissues. Prx II is also localized to the cytosol and is highly expressed in red blood cells (RBCs), whereas Prx III is restricted to mitochondria, and Prx IV is present in the endoplasmic reticulum and the extracellular space [3].

We previously cloned murine Prx I, first termed MSP23 (macrophage stress protein 23 kDa), from peritoneal macrophages as a major electrophile-inducible protein [7]. We showed that the stress-induced gene expression of Prx I is

☆ *Abbreviations:* Prx I, peroxiredoxin I; EPR, electron paramagnetic resonance; L-band EPR, low frequency EPR; carbamoyl-PROXYL, 3-carbamoyl-2,2,5,5-tetramethylpyrrolidine-1-oxyl; Fe-NTA, ferric-nitrilotriacetate; AST, aspartate aminotransferase; ALT, alanine aminotransferase; ROS, reactive oxygen species; RBC, red blood cells; MSP23, macrophage stress protein 23 kDa; PAG, proliferation-associated gene; Nrf2, NF-E2-related transcription factor 2.

* Corresponding author. Fax: +81 29 853 3061.
E-mail address: teishii@md.tsukuba.ac.jp (T. Ishii).

[1] Authors contributed to this work equally.

0006-291X/$ - see front matter © 2005 Elsevier Inc. All rights reserved.
doi:10.1016/j.bbrc.2005.10.192

controlled by NF-E2-related transcription factor 2 (Nrf2) [8]. Nrf2 is essential for regulating the ARE/EpRE-mediated expression of detoxifying enzymes such as NQO1 and glutathione *S*-transferases (GSTs), which are induced by dietary BHA in the liver and intestine [9]. Prx I is expressed at high levels in the liver, kidney, and small intestine, and dietary BHA increases Prx I expression in the mouse liver and proximal small intestine in a manner similar to the induction of GSTs [10]. These results suggest that Prx I is important in metabolically active tissues. However, a previous study by Neumann et al. [11] reported that Prx $I^{-/-}$ mice are viable and fertile, and have no apparent defects until 9 months of age, although the embryonic fibroblasts derived from Prx $I^{-/-}$ mice are sensitive to H_2O_2. They showed that the Prx $I^{-/-}$ mice gradually develop severe hemolytic anemia and several malignant cancers after 9 months of age.

In this study, we generated Prx $I^{-/-}$ mice by gene trapping and evaluated the antioxidant role of Prx I in vivo. To minimize the secondary effects of the Prx I deficiency, we used young mice, 9- to 14-week old, which are apparently normal. We injected ferric-nitrilotriacetate (Fe-NTA) into the mice, and evaluated the oxidative damage to tissues such as the liver and kidney that occurred as the result of hydroxyl radical production [12]. It is well known that a single intraperitoneal injection of Fe-NTA into experimental animals dose-dependently induces a transient elevation in the plasma iron concentration, the lipid peroxidation in the liver, and the blood levels of AST (aspartate aminotransferase), ALT (alanine aminotransferase), ALP (alkaline phosphatase), and γ-GTP (γ-glutamyl transpeptidase) [13]. We found that Prx $I^{-/-}$ mice showed higher sensitivity than wild-type mice to Fe-NTA.

The recent development of low-frequency electron paramagnetic resonance (EPR) using a stable paramagnetic spin probe has enabled researchers to estimate both the oxidative stress level and the antioxidant status of small animals in a noninvasive manner [14,15]. In this method, a paramagnetic species is injected into animals, and its spatial distribution and concentration are then monitored in vivo [16,17]. The stable paramagnetic spin probe 3-carbamoyl-2,2,5,5-tetramethylpyrrolidine-1-oxyl (carbamoyl-PROXYL) is converted to its corresponding hydroxylamine by one-electron reduction and loses its EPR signal in organs. Consequently, the reducing activity against radicals in the organ can be evaluated by EPR imaging analysis [18]. We showed previously that the combination of Nrf2 deficiency and aging markedly prolongs the half-life of nitroxyl radical disappearance [19]. In this study, using EPR imaging analysis, we found that Prx $I^{-/-}$ mice showed a diminished capacity to reduce carbamoyl-PROXYL compared with wild-type mice.

Materials and methods

Materials. Carbamoyl-PROXYL was purchased from Aldrich Chemical (Milwaukee, WI). Ferric nitrate enneahydrate and sodium carbonate were from Wako Biochemicals (Osaka); nitrilotriacetic acid (NTA) disodium salt was from Nacalai Tesque (Kyoto). All other chemicals were obtained from Sigma (St. Louis, MO) through Sigma Japan (Tokyo, Japan). All chemical reagents were of the highest purity commercially available.

Prx I-deficient mice. Embryonic stem (ES) cells with a retroviral gene trap vector inserted into the Prx I locus (OmniBank No. OST422296) were selected from the OmniBank library [20] by Lexicon Genetics Incorporated (The Woodlands, TX). Sequence analysis showed that the gene trap was inserted into intron 3 of the Prx I gene (Fig. 1A). The Prx I-targeted ES cells were microinjected into C57BL/6 blastocysts and then transferred to a foster mother to generate chimeric animals in collaboration with Lexicon Genetics Incorporated. Chimeric males were mated with C57BL/6 females, and F1 agouti pups were analyzed for the presence of the transgene by PCR analysis of the tail genomic DNA (Fig. 1B) using the following primers: Prx I: (A) 5′-CTAATATCTAATATGCACTGGT GAGC-3′; (B) 5′-ATGGTGCGCTTGGGATCTGATATT-3′; LTR: (C) 5′-AAATGGCGTTACTTAAGCTAGCTTGC-3′.

Prx I heterozygous mutant (Prx $I^{+/-}$) mice were crossed to obtain Prx I homozygous mutant (Prx $I^{-/-}$) mice. After crosses between the heterozygous mutant, Prx $I^{-/-}$, Prx $I^{+/-}$, and Prx $I^{+/+}$ offspring were born at a normal Mendelian ratio (1:2:1), indicating that the Prx I gene is not essential for embryonic development. The strain was crossed with C57BL/6 mice for more than 7 generations before analysis. Mice were kept under specific pathogen-free conditions in an environmentally controlled clean room at the Laboratory Animal Resource Center, University of Tsukuba. They were housed at an ambient temperature of 24 °C with a daily cycle of 12 h light and darkness (7:00 to 19:00). The mice had free access to drinking water and standard chow containing 0.9% calcium and 0.7% phosphorus (MF: Oriental Yeast; Tokyo Japan). For the measurement of peripheral blood parameters, female Prx $I^{-/-}$ and wild-type mice aged around 35 weeks were used ($n = 6$). For EPR imaging, male Prx $I^{-/-}$ and wild-type mice aged around 9 weeks were used ($n = 6$). For the injection of Fe-NTA solution, female Prx $I^{-/-}$ and wild-type mice aged around 14 weeks were used ($n \geqslant 5$: three groups). All experiments were performed with permission from the Animal Experiment Committee, University of Tsukuba, and in accordance with the University of Tsukuba's Regulations on Animal Experiments and Japanese Governmental Law No. 105.

Northern blot analysis. Total RNAs isolated from mouse tissues by Isogen (Nippon Gene, Toyama, Japan) were denatured with formaldehyde, size-separated in a 1.0% agarose gel, blotted onto a Zeta-Probe GT membrane (Bio-Rad), and hybridized to a ^{32}P-labeled cDNA probe for murine Prx I (MSP23), as described [7]. To monitor the efficiency of RNA loading and transfer, 18S rRNA was used as an internal control. Autoradiography was performed using the BAS-5000 image analysis system (FUJI FILM).

Western blotting. Tissue or cell proteins were solubilized with SDS-sample buffer (without dye or 2-mercaptoethanol) containing a protease inhibitor cocktail (Sigma). Protein concentrations were estimated using the BCA protein assay (Pierce). Proteins (25 μg/well) were separated by 12% SDS–polyacrylamide gel electrophoresis and then transferred onto a polyvinylidene fluoride (PVDF) membrane. We used two polyclonal rabbit sera raised, respectively, against a recombinant mouse Prx I fragment (a.a. 29–199) [7] and rat liver Prx I [21]. The former (lot No. 246) reacted with both Prx I and Prx II, and the latter (lot No. 232) reacted preferentially with Prx I. To detect immunoreactive proteins, we used horseradish peroxidase-conjugated anti-rabbit IgG and ECL blotting reagents (Amersham Pharmacia Biotech).

Preparation and injection of Fe-NTA solution. Fe-NTA solution was prepared immediately before use by the method of Awai et al. [22] with slight modification. Ferric nitrate enneahydrate and NTA disodium salt were each dissolved in deionized water to prepare 300 and 600 mM solutions, respectively. These solutions were then mixed at a volume ratio of 1:2 (molar ratio, 1:4) with magnetic stirring at room temperature. The pH was adjusted with sodium carbonate to 7.4. Each group of 5–8 mice received injections intraperitoneally of either physiological saline or Fe-NTA solution (5 mg Fe/kg body weight) and were sacrificed after 4 or

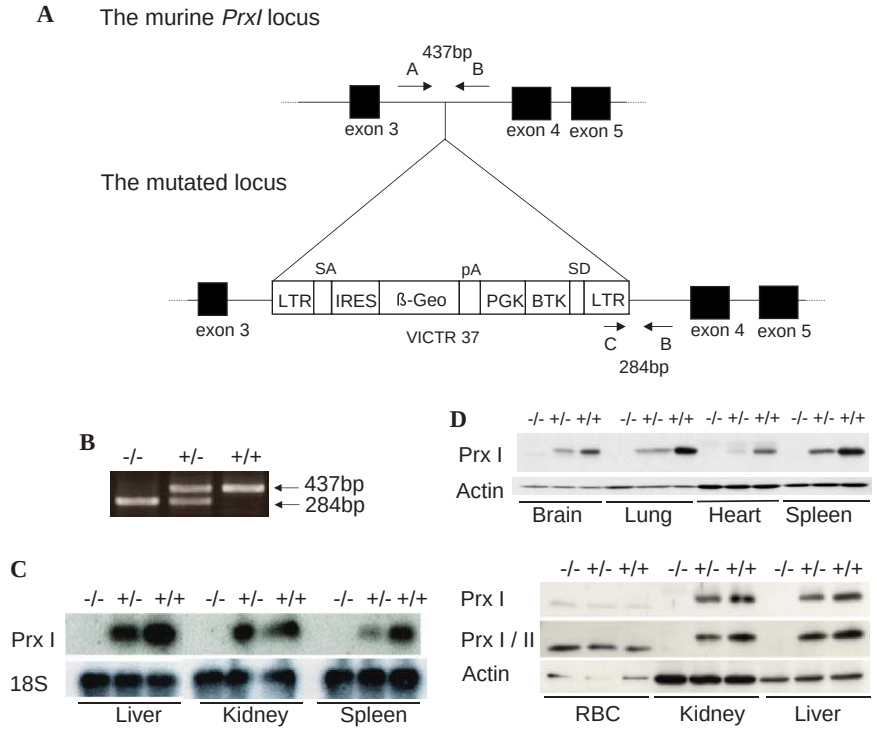

Fig. 1. Gene targeting of the Prx I locus. (A) Map of the *Prx 1* locus (upper panel) and mutated locus (lower panel). LTR, long terminal repeat; IRES, internal ribosome entry site; β-Geo, β-galactosidase-neomycin phosphotransferase fusion gene; pA, polyadenylation sequence; SA, splice acceptor sequence; SD, splice donor sequence; PGK, phosphoglycerate kinase 1 promoter; BTK, Bruton's tyrosine kinase. (B) PCR genotyping of DNA distinguishing Prx $I^{-/-}$, Prx $I^{+/-}$, and Prx $I^{+/+}$ male mice. (C) Northern blot analysis of tissues from Prx $I^{-/-}$, Prx $I^{+/-}$, and Prx $I^{+/+}$ mice using ^{32}P-labeled mouse Prx I and 18*S* rRNA cDNA as probes. (D) Western blot analysis of Prx I protein expression in various tissues. Two rabbit anti-sera, one highly specific to Prx I (Prx I, lot No. 232) and one cross-reactive with Prx I and II (Prx I/II, lot No. 246) were used for these immunoblots.

12 h. Blood was obtained from the abdominal aorta, and 300 μl serum from each animal was used for the analysis of aspartate aminotransferase (AST), alanine aminotransferase (ALT), and creatinine. The analysis was performed by SRL (Tokyo) using an automatic chemical analyzer (Hitachi).

Imaging study. Carbamoyl-PROXYL (200 mM, 3 ml/kg) was injected into animals subcutaneously, 15 min after pentobarbital anesthesia. Each mouse was then placed in a plastic holder and put into the EPR system so that its upper abdominal area was in the center; the bladder was outside of the resonator. Three-dimensional EPR images were constructed using the peak located in the lowest magnetic field of the triplet carbamoyl-PROXYL EPR signal, using ESR-CT version 1.183 software (JEOL, Tokyo, Japan). EPR conditions were as follows: field gradient, 2.0 mT/cm; changing direction, 20° steps (provides nine spectra for each projection); magnetic field, 37.0 ± 5.0 mT; microwave power, 0.25 mW; and modulation width, 0.1 mT; time constant, 0.03 s; scanning time for each spectrum, 1 s; total scanning time, approximately 210 s; and microwave frequency, ~1100 MHz. Details for the EPR imaging hardware system and measuring methods were described in our previous reports [19].

On the obtained EPR image, a square area encompassing each organ was determined from the first image after the carbamoyl-PROXYL injection. Unlike nuclear magnetic resonance imaging (MRI), the shape of each domain in EPR imaging is determined by the signal intensity in the area rather than the organ outline. Therefore, we needed to determine carefully the area corresponding to each organ, and the organ area was confirmed not only with one cross-sectional image but with all 3D images (i.e., the *ZY*, *XY*, and *XZ* planes).

Statistical analysis. Significant differences between the groups of mice were analyzed by the unpaired Student's *t* test. The analyses were performed using the StatView 5.0 statistical software package (SAS Institute, Cary, NC, USA).

Results

Prx $I^{-/-}$ mice exhibit normal blood profiles

Prx $I^{-/-}$ mice were normal in appearance, blood parameters, and spleen and body weights, up to 35 weeks of age (Table 1). Northern and Western blot analyses revealed that the Prx I mRNA and protein product were absent in tissues from Prx $I^{-/-}$ mice, and expressed at roughly half their wild-type amounts in Prx $I^{+/-}$ mice (Figs. 1C and D). Notably, we could not detect Prx I in the RBCs from mice of any genotype using the anti-Prx I serum (lot No. 232) that was highly specific to Prx I (Fig. 1D lower panel). When we used another anti-Prx I serum (lot No. 246) that cross-reacted with Prx II, which appeared as a slightly smaller band than Prx I in SDS–PAGE, we detected normal levels of Prx II in the RBCs from the mice of all the genotypes (Fig. 1D lower panel). The expression levels of Cu,Zn-SOD and Mn-SOD in the liver and kidney determined by immunoblot analysis did not differ between the Prx $I^{+/+}$ and Prx $I^{-/-}$ mice (not shown).

Prx $I^{-/-}$ mice are sensitive to Fe-NTA

Fe-NTA injection is used as an animal model of iron overload. Fe-NTA uptake in the liver causes membrane lipid peroxidation and subsequently produces a transient

Table 1
Blood parameters and body weight of Prx $I^{+/+}$ and Prx $I^{-/-}$ mice

	Prx $I^{+/+}$	Prx $I^{-/-}$
RBC ($\times 10^6$ per μl)	8.1 ± 0.2	8.1 ± 0.3
Hematocrit (%)	44.5 ± 1.3	44.9 ± 1.6
Hemoglobin (g dl^{-1})	12.1 ± 0.3	12.2 ± 0.4
Reticulocytes (‰)	22.3 ± 5.0	22.2 ± 2.7
WBC ($\times 10^3$ per μl)	3.8 ± 1.4	2.7 ± 0.6
Platelets ($\times 10^4$ per μl)	140.7 ± 9.7	123.2 ± 11.2
Body weight (g)	25.0 ± 0.9	23.0 ± 1.3
Spleen (g)	0.12 ± 0.04	0.09 ± 0.01

Peripheral blood was obtained from Prx $I^{-/-}$ and age-matched (35 weeks) Prx $I^{+/+}$ female mice. Values denote means ± SD ($n = 6$).

liberation of liver cell enzymes [13,23]. We used Fe-NTA injection to compare the tissue sensitivities of Prx $I^{-/-}$ vs. Prx $I^{+/+}$ mice to oxidative stress. After the intra-peritoneal injection of Fe-NTA, the serum levels of AST, ALT, and creatinine at 4 and 12 h were measured, and the results are shown in Table 2. The levels of AST, ALT, and creatinine were similar in the Prx $I^{-/-}$ and Prx $I^{+/+}$ mice before the Fe-NTA treatment. The creatinine level did not change significantly in either type of mouse 4 and 12 h after treatment, suggesting there was no extensive functional defect in the kidney. In the Prx $I^{+/+}$ mice, both AST and ALT increased significantly 4 h after the Fe-NTA injection and returned to basal levels by 12 h. In the Prx $I^{-/-}$ mice, however, these enzymes increased to a level higher than that seen in the Prx $I^{+/+}$ mice after 4 h and remained elevated at 12 h. These findings indicate that the Prx $I^{-/-}$ mice are more sensitive than normal to Fe-NTA-mediated tissue damage.

Prx $I^{-/-}$ mice have a lower capacity to eliminate carbamoyl-PROXYL

To monitor the radical reducing activity of Prx $I^{-/-}$ mice in vivo, we performed EPR imaging analysis using a synthetic radical, carbamoyl-PROXYL. After the subcutaneous injection of carbamoyl-PROXYL, the EPR signals were monitored from 8 to 25 min. Fig. 2A shows typical EPR images of trans-axial sections (~0.3-mm thick) of the upper abdominal area of a Prx $I^{+/+}$ mouse 8 min after the carbamoyl-PROXYL injection. Square areas corresponding to the liver or kidneys were determined from the image (Fig. 2B). In the succeeding images, the areas with the same shape and size as that of the organ in the first image were determined, and the signal intensities from those areas were measured. The distribution of carbamoyl-PROXYL to each organ was confirmed using organ homogenates, as described previously [24].

The time-dependent change in EPR image was monitored for both Prx $I^{+/+}$ and Prx $I^{-/-}$ mice (Fig. 2C), and the signal intensity in each organ area was calculated. The decay plots of the nitroxyl radicals were fitted to straight lines on a semi-logarithmic scale (Fig. 3A shows typical cases), as reported previously [25]. The half-lives (means ± SD) in the liver and kidneys of Prx $I^{-/-}$ mice were 14.5 ± 4.3 and 14.7 ± 5.2 min, and those in Prx $I^{+/+}$ mice were 8.1 ± 1.1 and 7.6 ± 0.9 min, respectively (Fig. 3B). The statistical analysis showed that the free radicals remained longer in the Prx $I^{-/-}$ mice than in the Prx $I^{+/+}$ mice, suggesting that the Prx $I^{-/-}$ mice have a lower capacity to eliminate them.

Table 2
AST, ALT, and creatinine concentration in serum after intraperitoneal injection of Fe-NTA

		Untreated	Fe-NTA	
			4 h	12 h
AST (IU/L)	Prx $I^{+/+}$	69.5 ± 25.5	113.4 ± 19.3	66.1 ± 12.9
	Prx $I^{-/-}$	69.4 ± 25.1	$176.3 \pm 62.5^{*}$	$115.5 \pm 57.8^{**}$
ALT (IU/L)	Prx $I^{+/+}$	31.1 ± 24.2	39.2 ± 11.5	27.0 ± 6.5
	Prx $I^{-/-}$	34.8 ± 10.9	$65.2 \pm 18.5^{*}$	$44.3 \pm 10.7^{**}$
Creatinine (mg/dl)	Prx $I^{+/+}$	0.14 ± 0.03	0.10 ± 0.01	0.12 ± 0.01
	Prx $I^{-/-}$	0.13 ± 0.01	0.11 ± 0.01	0.10 ± 0.02

AST and ALT were significantly increased in Prx $I^{-/-}$ male mice. Values denote means ± SD ($n = 5$–8).
* $P < 0.05$ vs. Prx $I^{+/+}$.
** $P < 0.01$.

Discussion

In this study, we generated Prx I-deficient mice by gene trapping and examined their phenotype, noting a lack of apparent defects even at the age of 35 weeks (Table 1). We used young mice aged 9–14 weeks and examined the role of Prx I expressed in tissues under oxidative stress by comparing wild-type and mutant mice. We examined the tissue damage caused by the hydroxyl radical-producing agent, Fe-NTA, and the ability of mice to reduce the synthetic radical, carbamoyl-PROXYL. We found that the mutant Prx I mice exhibited (i) a higher sensitivity to Fe-NTA-induced oxidative tissue damage (see Table 2) and (ii) a lower ability to reduce carbamoyl-PROXYL in the liver and kidney (Figs. 2 and 3) than wild-type mice. These results clearly show that Prx I plays a role in protecting tissue from Fe-catalyzed oxidative damage and in reducing this radical compound in these tissues.

Notably, the tissue damage caused by Fe-NTA and estimated by the serum AST and ALT levels in Prx $I^{-/-}$ mice was only about twofold higher than that in Prx $I^{+/+}$ mice under the experimental conditions employed (Table 2). This result suggests that antioxidant enzymes and systems other than Prx I may also significantly protect tissues against Fe-NTA, although Prx I has high affinity for H_2O_2 and is expressed highly in tissues such as the liver and kidney. The role of Prx in protection from hydroxyl radicals [26], thiyl radicals, and oxidized thiyl radical anions [27] in the in vitro system is due at least in part to its peroxidase activity [28]. Since the presence of H_2O_2 is necessary for the Fe-catalyzed generation of hydroxyl radicals, Prx I contributes to the prevention of tissue damage caused by Fe-NTA through, at least in part, the elimination of H_2O_2. This is consistent with the observation that

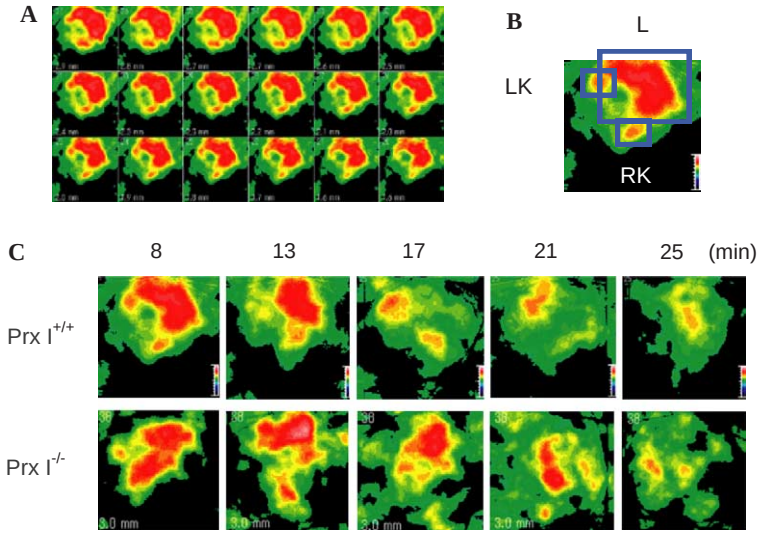

Fig. 2. EPR images of the upper abdominal area of a mouse. (A) A typical series of trans-axial sectional images of a wild-type mouse 8 min after the carbamoyl-PROXYL injection. High signal intensity is indicated in red and low intensity in green. The image in the top left corner shows the most cephalic section, and the image in the bottom right corner shows the most caudal section of the abdomen. The thickness of each slice was ~0.3 mm. (B) The high-intensity area in the center of each tiled image represents the liver (L). The high-intensity area adjoining the liver on the left abdominal side represents the left kidney (LK), and the area on the right side of the liver represents the right kidney (RK). (C) Typical EPR images of the upper abdomen of Prx $I^{+/+}$ (upper panel) and Prx $I^{-/-}$ mice (lower panel) at 8, 13, 17, 21, and 25 min after the carbamoyl-PROXYL injection. EPR conditions are described in Materials and methods.

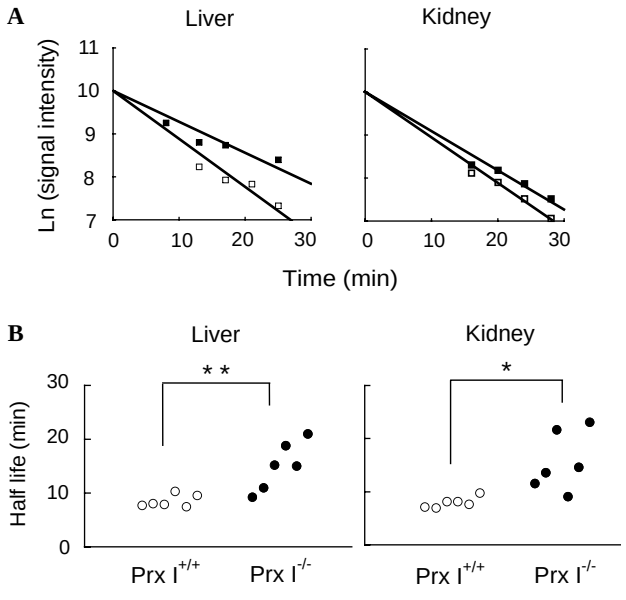

Fig. 3. Analysis of the nitroxyl radical decay in the kidney and liver of Prx $I^{+/+}$ and Prx $I^{-/-}$ mice. (A) Typical time-dependent signal decay plots from a Prx $I^{-/-}$ mouse (filled squares) and a Prx $I^{+/+}$ mouse (open squares). (B) The half-lives in the renal and hepatic areas of Prx $I^{+/+}$ (open circles) and Prx $I^{-/-}$ (filled circles) mice are shown. Each circle represents the calculated value from a different mouse. The half-lives of carbamoyl-PROXYL decay in the liver and kidney were significantly prolonged in the Prx $I^{-/-}$ mice compared with Prx $I^{+/+}$ mice. $^{**}P < 0.01$; $^{*}P < 0.05$.

embryonic fibroblasts from Prx $I^{-/-}$ mice are sensitive to H_2O_2 in vitro [11].

This study also shows that Prx I contributes to the radical reducing activity in the liver and kidney, where it is highly expressed. The metabolic disappearance of EPR signals from carbamoyl-PROXYL occurs as a result of one-electron reduction. Nitroxide spin probes do not react chemically with small thiol compounds; however, GSH has been shown to have a significant role in the bioreduction of nitroxides [29]. In addition to GSH, cytochrome P-450 reductase and the mitochondrial electron transport system are known to be involved in the reduction of nitroxide radicals. In our previous study, using Nrf2-deficient mice, we suggested that the delayed EPR signal decay in those mice compared with wild-type mice was due to diminished antioxidant activity in both the liver and kidney [19]. The present results confirm that Prx I contributes to tissue antioxidant activity reducing the carbamoyl-PROXYL radical, even though Prx I cannot react directly with the radical compound.

Neumann et al. [11] reported that Prx I-deficient mice show significant defects in hematological parameters and severe anemia after 9 months. We have not yet confirmed the occurrence of anemia in Prx $I^{-/-}$ mice aged over 9 months, but if it occurs, it could be a secondary effect of the Prx I deficiency. Notably, RBCs contain Prx II (also known as NKEF B, Calpromotin, or Torin) as the major Prx and express very little Prx I (Fig. 1) [30]. RBCs from our Prx $I^{-/-}$ mice showed normal Prx II expression levels (Fig. 1). It is reasonable to find that young Prx II-deficient mice show defects in hematologic parameters and splenomegaly [31]. The pathogenesis of the severe anemia observed in the aged Prx $I^{-/-}$ mice of Neumann [11] is less clear and should be carefully investigated.

In summary, our results from both Fe-NTA injection and the EPR imaging of carbamoyl-PROXYL indicate an in vivo role for Prx I in the protection of tissues from ROS. Since oxidative stress causes liver dysfunction,

including carcinoma [32], nonalcoholic fatty liver disease [33], and alcoholic liver diseases [34], Prx I-deficient mice provide a valuable tool for elucidating the role of antioxidant pathways in these pathophysiological processes.

Acknowledgments

We thank Professor G.E. Mann for his comments on this study. This work was supported by grants from University of Tsukuba Research Projects, and from the Japanese Society for Promotion of Science to T.I. (15310033), T.Y. (16591983), A.H. (15790427), and H.Y. (14370656).

References

[1] B. Halliwell, J. Gutteridge, Free Radicals in Biology and Medicine, second ed., Clarendon Press, Oxford, 1989.
[2] H.Z. Chae, S.J. Chung, S.G. Rhee, Thioredoxin-dependent peroxide reductase from yeast, J. Biol. Chem. 269 (1994) 27670–27678.
[3] S.G. Rhee, S.W. Kang, T.S. Chang, W. Jeong, K. Kim, Peroxiredoxin, a novel family of peroxidases, IUBMB Life 52 (2001) 35–41.
[4] B. Hofmann, H.J. Hecht, L. Flohe, Peroxiredoxins, Biol. Chem. 383 (2002) 347–364.
[5] Z.A. Wood, E. Schroder, J. Robin Harris, L.B. Poole, Structure, mechanism and regulation of peroxiredoxins, Trends Biochem. Sci. 28 (2003) 32–40.
[6] S.G. Rhee, S.W. Kang, W. Jeong, T.S. Chang, K.S. Yang, H.A. Woo, Intracellular messenger function of hydrogen peroxide and its regulation by peroxiredoxins, Curr. Opin. Cell Biol. 17 (2005) 183–189.
[7] T. Ishii, M. Yamada, H. Sato, M. Matsue, S. Taketani, K. Nakayama, Y. Sugita, S. Bannai, Cloning and characterization of a 23-kDa stress-induced mouse peritoneal macrophage protein, J. Biol. Chem. 268 (1993) 18633–18636.
[8] T. Ishii, K. Itoh, S. Takahashi, H. Sato, T. Yanagawa, Y. Katoh, S. Bannai, M. Yamamoto, Transcription factor Nrf2 coordinately regulates a group of oxidative stress-inducible genes in macrophages, J. Biol. Chem. 275 (2000) 16023–16029.
[9] K. Itoh, T. Chiba, S. Takahashi, T. Ishii, K. Igarashi, Y. Katoh, T. Oyake, N. Hayashi, K. Satoh, I. Hatayama, M. Yamamoto, Y. Nabeshima, An Nrf2/small Maf heterodimer mediates the induction of phase II detoxifying enzyme genes through antioxidant response elements, Biochem. Biophys. Res. Commun. 236 (1997) 313–322.
[10] T. Ishii, K. Itoh, J. Akasaka, T. Yanagawa, S. Takahashi, H. Yoshida, S. Bannai, M. Yamamoto, Induction of murine intestinal and hepatic peroxiredoxin MSP23 by dietary butylated hydroxyanisole, Carcinogenesis 21 (2000) 1013–1016.
[11] C.A. Neumann, D.S. Krause, C.V. Carman, S. Das, D.P. Dubey, J.L. Abraham, R.T. Bronson, Y. Fujiwara, S.H. Orkin, R.A. Van Etten, Essential role for the peroxiredoxin Prdx1 in erythrocyte antioxidant defence and tumour suppression, Nature 424 (2003) 561–565.
[12] K. Ikeda, F. Sun, K. Tanaka, S. Tokumaru, S. Kojo, Increase of lipid hydroperoxides in the rat liver and kidney after administering ferric nitrilotriacetate, Biosci. Biotechnol. Biochem. 62 (1998) 1438–1439.
[13] K. Yamaoka, T. Nomura, K. Iriyama, S. Kojima, Inhibitory effects of prior low dose X-ray irradiation on Fe(3+)-NTA-induced hepatopathy in rats, Physiol. Chem. Phys. Med. NMR 30 (1998) 15–23.
[14] T. Yoshimura, H. Yokoyama, S. Fujii, F. Takayama, K. Oikawa, H. Kamada, In vivo EPR detection and imaging of endogenous nitric oxide in lipopolysaccharide-treated mice, Nat. Biotechnol. 14 (1996) 992–994.
[15] Y. Miura, T. Ozawa, Noninvasive study of radiation-induced oxidative damage using in vivo electron spin resonance, Free Radic. Biol. Med. 28 (2000) 854–859.
[16] M.C. Krishna, N. Devasahayam, J.A. Cook, S. Subramanian, P. Kuppusamy, J.B. Mitchell, Electron paramagnetic resonance for small animal imaging applications, Ilar J. 42 (2001) 209–218.
[17] P. Kuppusamy, EPR spectroscopy in biology and medicine, Antioxid. Redox Signal 6 (2004) 583–585.
[18] H. Togashi, T. Matsuo, H. Shinzawa, Y. Takeda, L. Shao, K. Oikawa, H. Kamada, T. Takahashi, Ex vivo measurement of tissue distribution of a nitroxide radical after intravenous injection and its in vivo imaging using a rapid scan ESR-CT system, Magn. Reson. Imag. 18 (2000) 151–156.
[19] A. Hirayama, K. Yoh, S. Nagase, A. Ueda, K. Itoh, N. Morito, K. Hirayama, S. Takahashi, M. Yamamoto, A. Koyama, EPR imaging of reducing activity in Nrf2 transcriptional factor-deficient mice, Free Radic. Biol. Med. 34 (2003) 1236–1242.
[20] B.P. Zambrowicz, G.A. Friedrich, E.C. Buxton, S.L. Lilleberg, C. Person, A.T. Sands, Disruption and sequence identification of 2000 genes in mouse embryonic stem cells, Nature 392 (1998) 608–611.
[21] T. Ishii, T. Kawane, S. Taketani, S. Bannai, Inhibition of the thiol-specific antioxidant activity of rat liver MSP23 protein by hemin, Biochem. Biophys. Res. Commun. 216 (1995) 970–975.
[22] M. Awai, M. Narasaki, Y. Yamanoi, S. Seno, Induction of diabetes in animals by parenteral administration of ferric nitrilotriacetate. A model of experimental hemochromatosis, Am. J. Pathol. 95 (1979) 663–673.
[23] M. Awai, Pathogenesis and mechanism of iron overload: ferric nitrilotriacetate, hemosiderin, active oxygen, and carcinogenesis, Rinsho Ketsueki 30 (1989) 1115–1127.
[24] A. Hirayama, S. Nagase, A. Ueda, T. Oteki, K. Takada, M. Obara, M. Inoue, K. Yoh, K. Hirayama, A. Koyama, In vivo imaging of oxidative stress in ischemia–reperfusion renal injury using electron paramagnetic resonance, Am. J. Physiol. Renal Physiol. 288 (2005) F597–F603.
[25] H. Utsumi, K. Ichikawa, K. Takeshita, In vivo ESR measurements of free radical reactions in living mice, Toxicol. Lett. 82–83 (1995) 561–565.
[26] Y.S. Lim, M.K. Cha, H.K. Kim, T.B. Uhm, J.W. Park, K. Kim, I.H. Kim, Removals of hydrogen peroxide and hydroxyl radical by thiol-specific antioxidant protein as a possible role in vivo, Biochem. Biophys. Res. Commun. 192 (1993) 273–280.
[27] M.B. Yim, H.Z. Chae, S.G. Rhee, P.B. Chock, E.R. Stadtman, On the protective mechanism of the thiol-specific antioxidant enzyme against the oxidative damage of biomacromolecules, J. Biol. Chem. 269 (1994) 1621–1626.
[28] L.E.S. Netto, H.Z. Chae, S.W. Kang, S.G. Rhee, E.R. Stadtman, Removal of hydrogen peroxide by thiol-specific antioxidant enzyme (TSA) is involved with its antioxidant properties. TSA possesses thiol peroxidase activity, J. Biol. Chem. 271 (1996) 15315–15321.
[29] P. Kuppusamy, H. Li, G. Ilangovan, A.J. Cardounel, J.L. Zweier, K. Yamada, M.C. Krishna, J.B. Mitchell, Noninvasive imaging of tumor redox status and its modification by tissue glutathione levels, Cancer Res. 62 (2002) 307–312.
[30] T.H. Lee, S.U. Kim, S.L. Yu, S.H. Kim, D.S. Park, H.B. Moon, S. Dho, K.S. Kwon, H.J. Kwon, Y.H. Han, S. Jeong, S.W. Kang, H.S. Shin, K.K. Lee, S.G. Rhee, D.Y. Yu, Peroxiredoxin II is essential for sustaining life span of erythrocytes in mice, Blood 13 (2003) 13.
[31] T.H. Lee, S.U. Kim, S.L. Yu, S.H. Kim, S. Park do, H.B. Moon, S.H. Dho, K.S. Kwon, H.J. Kwon, Y.H. Han, S. Jeong, S.W. Kang, H.S. Shin, K.K. Lee, S.G. Rhee, D.Y. Yu, Peroxiredoxin II is essential for sustaining life span of erythrocytes in mice, Blood 101 (2003) 5033–5038.
[32] M. Yamada, M. Awai, T. Okigaki, Rapid in vitro transformation system for liver epithelial cells by iron chelate, Fe-NTA, Cytotechnology 3 (1990) 149–156.
[33] S. Gawrieh, E.C. Opara, T.R. Koch, Oxidative stress in nonalcoholic fatty liver disease: pathogenesis and antioxidant therapies, J. Investig. Med. 52 (2004) 506–514.
[34] D. Wu, A.I. Cederbaum, Alcohol, oxidative stress, and free radical damage, Alcohol Res. Health 27 (2003) 277–284.